Vortex-LES
White Paper

ABSTRACT - Mesoscale-microscale coupling has constituted one of the major challenges of the wind industry modeling subsector over the last few years. Wind resource datasets based on mesoscale numerical weather prediction models involve a mature technology that is drawing to a close because the set of approximations used for parameterizing the Planetary Boundary Layer do not remain valid at grid-resolutions of tens and hundreds of meters. Furthermore, the degree of development of the industry calls for new specifications such as turbulence, inflow angle, ramps, wind gusts, wind turbines, which cannot be resolved explicitly by means of a mesoscale model.

Over the last three years, Vortex has focused its research on overcoming the main limitations of the cutting-edge atmospheric model created by the National Center of Atmospheric Research (NCAR), the Weather Research and Forecasting - Large Eddy Simulation (WRF-LES): i) software efficiency , ii) lateral boundary conditions, iii) Terra Incognita and iv) performance of the surface layer parameterization. As a result of this successful investigation, the Vortex-LES model is capable of providing one year of 10-min time series at any site across the world.

This document includes a full description of the Vortex-LES methodology and an extended validation of wind speed (85 sites) and turbulence (50 sites) accross the world with different met-mast heights, topographic complexity, local weather regimes and climate features.

The study of wind speed includes a discussion of several time scales (10-min, hourly, daily and monthly), daily cycle, spatial distribution, seasonal behavior and more sophisticated analyses such as Weibull parameters, energy spectrum and wind direction.

Results for 10-min time series show a mean correlation of 0.683, which increases to 0.881 for monthly values. Vortex-LES performs a mean absolute error of 5.1% with respect to mean wind speed.

The analysis of turbulence focuses upon 10-min values for wind standard deviation and turbulence intensity. Wind standard deviation shows a mean absolute error of 1.3%.

Turbulence intensity is studied as a function of wind speed, as this field is necessary for IEC studies. The results show a mean error of around 1.8%.

VORTEX

Why Vortex-LES?

In terms of the estimation of wind resource at a given site, the most accurate method involves analysis based upon on-site measurements. These measurements consist of a set of anemometers and wind vanes distributed lengthwise on a meteorological tower (hereinafter, met-mast) covering different heights, in order to determine the wind profile (resource estimation, shear or wind veer, among others). More recently, the wind industry has started to include remote sensing techniques such as LIDARs or SODARs in search of a better characterization of the vertical profile.

Although this approach is the most accurate one, it presents some relevant limitations. On one hand, installation and maintenance of these instruments is expensive. On the other, wind resource estimation requires long-term datasets (10, 20 or even 30 years) that are unaffordable for developers or investors. Numerical Weather Prediction (NWP) models offer a good solution with regard to overcoming the limitations of observational data in terms of costs or availability.

Atmosphere is described by a set of high non-linear equations based on fundamental principles of physics: momentum, energy and mass conservation. NWP models are computer programs that solve these equations by means of mathematical methods and approximations. These programs are commonly known by weather prediction applications. However, apart from being used to analyze the future state of the atmosphere, NWP models may also be applied to the past, with the advantage that the atmospheric unpredictability is reduced by using past global measurements.

Global data-assimilation systems, the so-called reanalyses, use an atmospheric model to periodically ingest observational data (weather stations, soundings, satellite, buoys, radar, etc.), the output being a gridded set of model variables consistent with model dynamics and the information provided by the observations (Warner, 2010). Consequently, this kind of models constitutes an interesting tool for

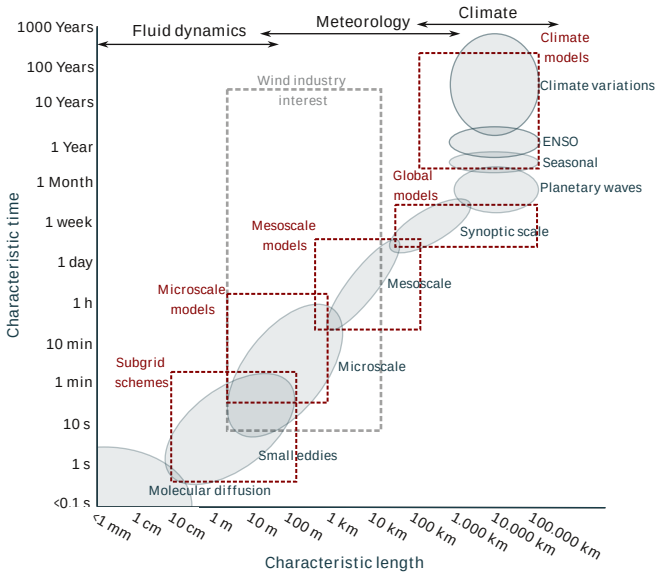

Fig. 1: Modeling strategies used for each meteorological scale. Mesoscale and microscale models are the common tools in wind resource assessment.

analyzing of the past state of the atmosphere, thus leading to a modeled evolution of the climate compatible with measurements. Nevertheless, this approach poses two important limitations. On the one hand, due to the lack of measurements before the 1980s, most of the reanalysis datasets are useless before this period, but this duration is sufficient for wind resource assessment applications. On the other hand, the process of generating a reanalysis involves high computational consumption and hence, it is only available for national or international institutions such as the National Aeronautics and Space Administration (NASA), the National Oceanic and Atmospheric Administration (NOAA) or the European Centre for Medium-Range Weather Forecasts (ECMWF), among others. Furthermore, these datasets present coarse grid resolutions for reducing computational time and storage specifications. Unfortunately, the spatial resolution provided by reanalyses is insufficient with regard to resolving the local effects required by the wind energy industry.

This limitation of reanalyses has been solved by coupling limited-area models, also known as mesoscale models (Fig. 1). These models enable a higher resolution, with the global model used as initial and lateral boundary conditions (LBC). Mesoscale models may consist of a single high-

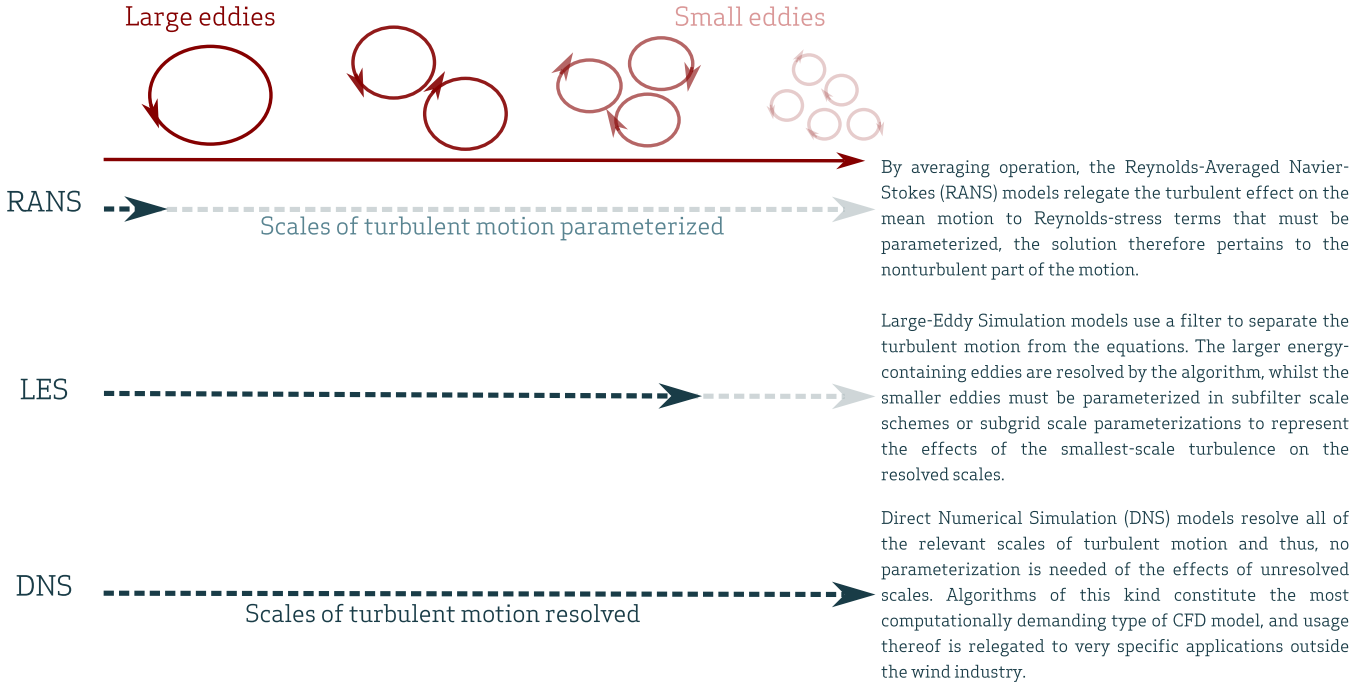

Fig. 2: Computational Fluid Dynamics (CFD) codes can be grouped in three categories: Reynolds-Averaged Navier-Stokes (RANS), Large-Eddy Simulation (LES) models and Direct Numerical Simulation (DNS) algorithms. LES is the most suitable tool for coupling in a NWP model.

resolution domain, or a set of multiple grids nested within each other with grid spacings that change abruptly by a factor of between three or five from parent to child domains (Warner, 2010). Under this approach, models describe the atmospheric processes with higher details reaching horizontal resolutions of 3 km in the last decade.

Nevertheless, the degree of description achieved by mesoscale models at 1-3 km is insufficient for a good description of microscale effects over the wind farm, such as local wind patterns or turbulence, because sub-kilometer eddies cannot be resolved by the governing equations and hence, they must be parameterized in terms of some empirical relationships or rough approximations (Fig. 1). In NWP models, turbulent processes are parameterized in the so-called Planetary Boundary Layer (PBL) schemes. These schemes distribute the surface fluxes within the PBL and they perform the vertical the diffusion due to turbulence in the free atmosphere. Turbulence is not the only physical process that needs to be parameterized; other physical processes such as solar and terrestrial radiative transfer, clouds and atmosphere-surface interaction must be simplified.

The solution to the lack of resolution is provided by engineering with Computational Fluid Dynamics (CFD) modeling (Fig. 2). These models are widely used to simulate the very fine motion scales of a fluid (e.g. water or air). However, the high degree of details of these codes involves high computational needs and hence, their application in the wind energy industry is limited to small regions, and particularly for determining the turbines layout, losses, loads or wakes.

NWP and CFD models are based on the same dynamical equations but they differ with regard to mathematical treatment. The former ones require a high simplification of the equations to include the previously introduced physical parameterizations. On the contrary, the latter models provide a more accurate description of the fluid motion (i.e. wind in this case) but they do not include other physical phenomena, negligible in fluid dynamics but relevant in the real atmosphere.

Consequently, they have been considered as independent tools for many years, necessary for covering the wind industry requirements. NWP models were used for large scale, whereas CFD codes were applied by engineers for small-scale studies.

> Vortex has worked in collaboration with scientists at the NCAR. Microscale simulations are already among us.

Among all CFD models, the LES type is the most suitable tool for resolving the turbulence motions within a mesoscale model. For many years, several researchers, such as Mirocha et al. (2014), Udina (2015) or Udina et al. (2016), have been working in this direction. However, these studies were limited to ideal cases due to the high computational demand and only some intrepid researchers have attempted to perform real experiments in a small number of case studies, such as Moeng et al. (2007) or Talbot et al. (2012).

Implementing a LES model within a mesoscale model presented four important challenges (Haupt et al., 2016, Montornès, 2016): i) LBC and spin-up for producing turbulence, ii) computational resources, iii) Terra Incognita and iv) surface parameterization. All of these will be explained in the following sections.

During the last four years, Vortex has been working in collaboration with scientists at the NCAR with the aim of solving these problems. We already avail of microscale simulations.

What is Vortex-LES?

Vortex-LES is a NWP-CFD on-line coupled framework based on the Weather Research and Forecasting (WRF) model powered by the Mesoscale and Microscale Meteorology Laboratory (MMM) of the NCAR. WRF is a state-of-the-art NWP model used both for research and prediction applications (Skamarock et al., 2008). In the case of wind resource assessment, the WRF model is a tool broadly used by many companies and research institutions.

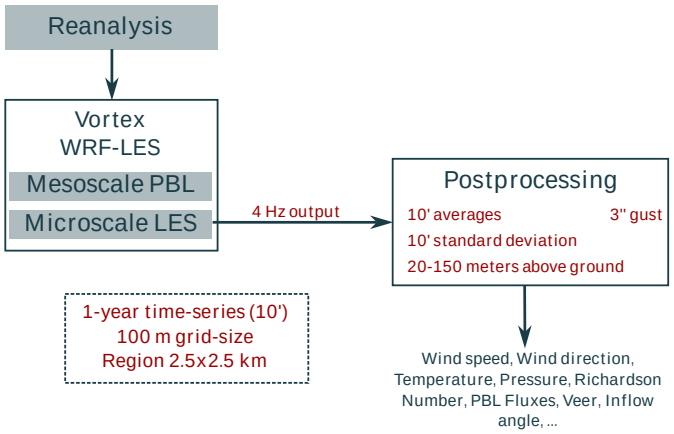

Fig. 3: Scheme of the Vortex-LES structure.

For microscale applications, the WRF model poses a CFD algorithm based on the LES approach. When WRF is coupled to the LES model the result is commonly known as WRF-LES model. This means that the simulation is run as usual but the turbulence parameterization is replaced by the LES model and hence, turbulent eddies are resolved. Under this approach, mesoscale and microscale are coupled in a seamless modeling chain.

Nevertheless, despite the fact that the WRF-LES code was extensively used for ideal experiments in the past, its implementation for real simulations was limited by the above mentioned series of challenges. Vortex has improved the source code in two ways: i) the problem of the LBC has been solved by including a perturbation in the potential temperature and ii) the source code of the WRF model has been improved through optimization of the computational needs. The modified version of the model is called Vortex-LES.

With the new version of the product, Vortex is able to provide high-res (100 m) modeled virtual datasets in any part of the world. The product consists of one year of 10-min time series at any point in a region of 6.25 km^2 around an initial set of coordinates and for any height between 50 m and 200 m above the ground. The simulation comprises a set of domains from reanalysis (ERA-5, CFSR or MERRA2) to microscale. The output for the main variables of interest for wind energy applications is saved every 0.25 s (i.e. 4 Hz) and finally aggregated into 10-min values (mean, standard deviation and higher order moments) as is shown in Fig 3.

Vortex-LES approach

The WRF-LES model has been extensively used for theoretical analyses as an initial trial for real applications in air quality or wind energy, for instance. However, four challenges have hindered the successful execution of real simulations:

i) LBC and spin-up issue

In a mesoscale simulation, turbulence processes cannot be resolved due to the spatial and temporal resolution. Consequently, these effects must be parameterized within a PBL scheme and thus, the solution of the NWP model belongs to the non-turbulent part of the flow. The information of the innermost mesoscale domain is used as input data (i.e. initial and LBC) for the outermost microscale domain. As a consequence, microscale domains start with horizontally homogeneous fields interpolated from the last mesoscale grid. These initial conditions inhibit the mechanical production of turbulence and hence, turbulence can only be developed by thermal effects. Therefore, the spin-up length necessary for producing turbulence increases, leading to a large increment in total computational time.

Furthermore, as turbulence is developed at the center of the domain, it is destroyed by the non-turbulent LBC, giving rise to unreliable results.

Several authors have attempted to address this problem, such as Muñoz-Esparza (2014, 2015), who mostly focused on ideal simulations. During the last four years, Vortex has worked on the implementation of the method proposed by Muñoz-Esparza in the WRF-LES model. This implementation also called for much research aimed at adapting the method to real case simulations.

Briefly, the method takes a set of points at the boundary of the microscale domain. These points are grouped in different cluster of grid-points. At each one of these clusters a perturbation of the potential temperature is applied. This perturbation is randomly created under a fixed amplitude in order to preserve the original solution of the atmospheric equations.

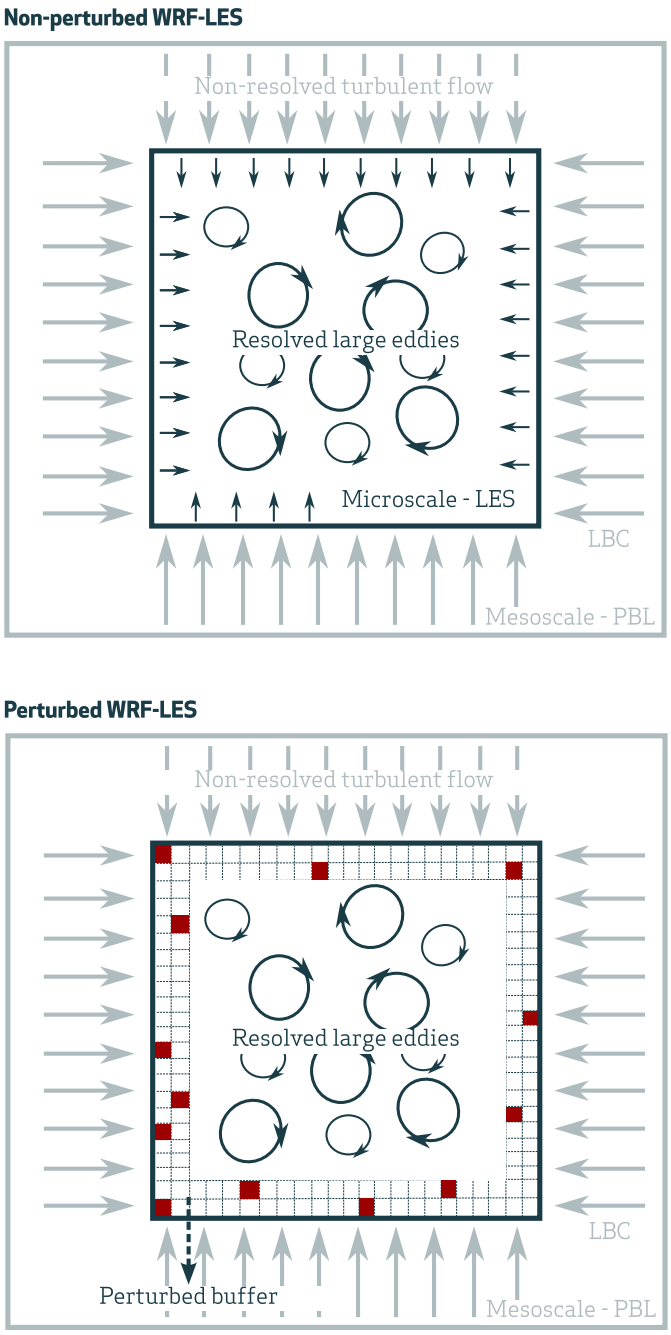

Fig. 4: Non-perturbed WRF-LES (top) cannot mantain the turbulence production because it is destroyed by the LBC. Perturbed WRF-LES case (bottom) based on Muñoz-Esparza (2014) and Vortex in-house research (Montornès, 2016).

This perturbation introduces horizontal and vertical inhomogeneities that accelerate production of mechanical turbulence, thus reducing spin-up time and the problem of the LBC. For a better understanding of the paper, further details are not provided here.

10-min average $< M >= \frac{1}{2400} \sum_0^{2399} m_i$

10-min standard deviation $\delta M^2 = \frac{1}{2400} \sum_0^{2399} (m_i - < M >)^2$

Wind components and module, temperature, pressure, density and moisture

Fig. 5: Post-processing of the high-frequency outcomes to 10-min values. Once the main variables are determined (wind components and module, temperature, pressure, etc), the derivated fields, such as the Richardon Number, wind direction or turbulence intensity, are computed.

ii) Computational costs

A mesoscale simulation with a horizon of 30 h consisting in a domain of 100 x 100 points, 50 vertical levels and a timestep of 30 s requires 1,800 million of integrations. This amount of computations is feasible with the current available resources.

However, at microscale the timestep must be reduced in order to ensure numerical stability. For example, in a simulation at 100 m of grid-resolution, the required timestep rounds off at between 0.25 and 0.5 s. Therefore, assuming the same domain configuration, the number of integrations increases to 216,000 million, i.e. a factor of 120. In other words, a microscale domain needs 120 times the computational power of a mesoscale one under the same conditions.

In addition, in the microscale the PBL scheme is replaced by a LES algorithm that requires more computation time for the integration of the equations.

Moreover, the WRF model is an open source model built by the contributions of the scientific community and this is a double edge sword. On the one hand, the code is widely used and has a large community of developers and users, which enriches the model. On the other hand, the code cannot be optimized and many resources are therefore wasted.

Another problem of WRF-LES outputs involves the storage needed for the model outcomes, which reaches more than 300 GB per day before the post-processing of the time series to 10-min values.

Vortex has been working on the code and on the compilation process, significantly reducing the computation resources and time needed to run a WRF-LES simulation.

Currently, WRF-LES at 100 m may be run in a reasonable time, thus constituting a feasible tool for the wind industry.

iii) Terra Incognita

As has previously been described, mesoscale approximations for turbulence breaks down progressively as grid resolution increases. There is a gray region in which current PBL schemes cannot be used but the LES approach is not yet valid. This region is typically known as Terra Incognita (Wyngaard, 2004). The formal definition is more complex than the one described here, but it is sufficient for the purposes of this paper.

The modeling community is making a great effort in this field, employing two different approaches to address the problem. On the one hand, some groups are attempting to extend PBL schemes to microscale with 3D solution (Kosovic, 2016). On the other, different groups are preparing some new schemes extending the LES solution to the mesoscale (Shin, 2015). At Vortex, we have been investigating different approaches but we do not yet have a final solution (Doubrawa, 2017b).

The challenge of the Terra Incognita has an effect on the structure of the energy spectrum as will be discussed in the results. Nevertheless, the results improve the current technology and thus, the Terra

Fig. 6: Example of Vortex-LES output for two weeks at 80 m above the ground. Measured values are represented in light green solid line, Vortex mesoscale product at 3 km is shown in red solid line and Vortex-LES in dark green solid line.

Incognita solution may be considered as a higher-order improvement for the coming years.

iv) Surface layer schemes and SGS

Surface layer schemes are physical parameterizations that consider heat, mass and momentum exchange between the surface and the atmosphere. Schemes of this kind were developed in the 1990s when most of the PBL parameterizations were developed. The set of approximations used in a mesoscale simulation is therefore no longer valid in microscale runs. As a consequence, in some situations the surface fluxes produce unrealistic patterns (Montornès, 2017).

This problem has been addressed during the last months and it will be explained in future contributions.

Post-processing

The results of Vortex-LES are saved at a frequency of 4 Hz (i.e. 0.25 s). This amount of data is collapsed into 10-min fields: average, standard deviation and fluxes.

Fig. 5 provides a description of the process used to obtain the 10-min outcomes (wind components and module, temperature, pressure, air density and moisture). Fig. 6 shows an example of the Vortex-LES outcomes at 10-min intervals for two weeks.

Moreover, using high frequency outputs is useful for an evaluation of the wind gust by way of a sonic anemometer as opposed to parameterizations, as occurs at the mesoscale.

A sample of 10-min outcomes at 4 Hz consists of 2,400 values. This interval is divided into 3-seconds intervals. For each interval, the mean value is computed providing 800 values of 3-second averages. Finally, the highest value within these 800 averages is sought and assigned as the wind gust in that 10-min interval.

> *Vortex-LES outcomes are saved at a frequency of 4 Hz (i.e. 0.25 s).* This amount of data is collapsed into 10-min fields: average, standard deviation and fluxes.

Fig. 7: Map of the sites used for the Vortex-LES product validation. Details of the sites are not presented due to confidential agreements.

Vortex-LES results are provided for a final region of 2.5 x 2.5 km, from surface to 200 m. Note that this region is smaller than the original grid due to the perturbation introduced in the boundaries (Fig. 4).

> *A thorough validation of 1-year time series at 85 sites for wind speed and 50 for turbulence around the world.*

Vortex-LES validation: Methodology

The Vortex-LES approach has been subjected to a rigorous validation process in order to evaluate the accuracy, reliability and potentialities of this new technology. The validation involves the analysis of the results of 1-year time series at 85 real sites for wind speed performance and 50 for turbulence skills (Fig. 7). The difference between the number of sites for wind speed and for turbulence studies responds to the availability of observational data.

Clients do not generally provide us with data on wind standard deviation or turbulence intensity. For this reason, these variables are validated in a lower number of sites.

Due to confidential agreements, the site measurements and names used in this validation are not revealed in the present white paper.

The sites used in the present white paper cover different geographical regions around the world presenting different degrees of complexity.

In the case of wind speed, there are 2 offshore sites (2% of the total), 32 flat-terrain sites (38%), 28 complex-terrain sites (33%) and 23 forested sites (27%). In geographical terms (Fig. 7), 19% of the sites are found in the Tropics, 76% in Mid-latitude regions and 5% in Polar areas.

For turbulence analyses, the selected sites constitute a subset of the aforementioned sites with the following features: 2 offshore sites (4%), 18 flat-terrain sites (36%), 19 complex-terrain sites (38%) and 11 forested sites (22%).

In order to provide a reliable validation for the industry, selected sites cover a wide range of met-mast heights from 50 m to 120 m.

The validation of wind speed time series shows a high dependence on the geographical features as well as climatological properties.

One site metrics

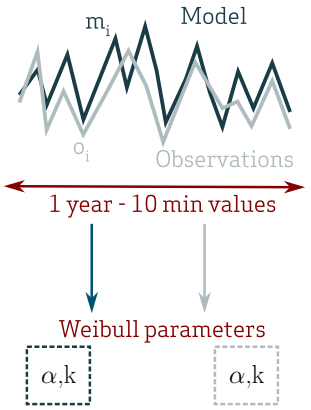

$$\text{Bias} = \frac{1}{T}\sum_{i=1}^{year} m_i - o_i$$

$$\text{RMSE} = \frac{1}{T}\sqrt{\sum_{i=1}^{year}(m_i - o_i)^2}$$

$$R^2 = \frac{Covariance(m,o)}{Variance(m)Variance(o)}$$

Normalization

Wind speed T =1 year<WS>

Wind standard deviation T =1 year<WSD>

$$\text{Error}_{\alpha,k} = \alpha, k_{model} - \alpha, k_{observations}$$

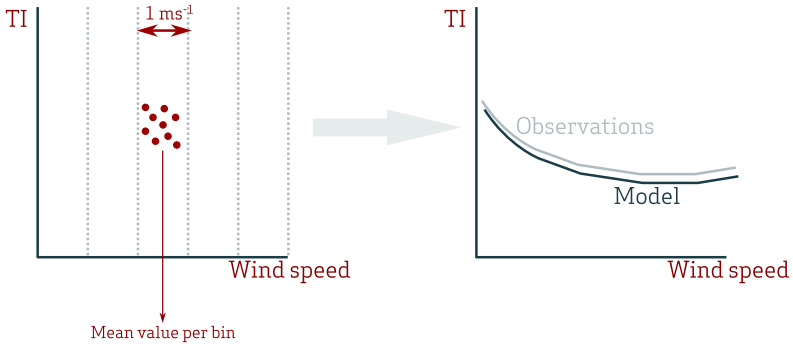

Metrics

MAE weighted by Weibull $\text{MAE}_w = \sum_{i=1}^{bins} f_i |TI_{m,i} - TI_{o,i}|$

MAE at bin 15 ms^{-1} $\text{MAE}_{15} = |TI_{m,15} - TI_{o,15}|$

All sites metrics

M is the number of sites

Weibull parameters

$$\text{ME}_{\alpha,k} = \frac{1}{M}\sum_{i=1}^{M} Error_{\alpha,k,i}$$

Mean Bias (MB)

$$\text{MB} = \frac{1}{M}\sum_{i=1}^{M} Bias_i$$

Mean Absolute Bias (MAB)

$$\text{MAB} = \frac{1}{M}\sum_{i=1}^{M} |Bias_i|$$

Mean Absolute RMSE (MRMSE)

$$\text{MRMSE} = \frac{1}{M}\sum_{i=1}^{M} RMSE_i$$

Mean Absolute R^2 (MR^2)

$$\text{MR}^2 = \frac{1}{M}\sum_{i=1}^{M} R^2$$

Mean MAE_w (MMAE_w)

$$\text{MMAE}_w = \frac{1}{M}\sum_{i=1}^{M} MAE_{w,i}$$

Mean MAE_{15} (MMAE_{15})

$$\text{MMAE}_{15} = \frac{1}{M}\sum_{i=1}^{M} MAE_{15,i}$$

Fig. 8: Metrics used in this validation. The upper plot shows the validation for a single site, while the lower figure illustrates the process for summarizing the resolt among a large number of met-masts.

The validation of this new product focuses on three variables: wind speed, wind standard deviation and turbulence intensity. Although they are not independent variables, they have been chosen due to their relevance in the wind industry and in order to demonstrate the robustness of this new model.

For wind speed time series, Bias, Root Meat Squared Error (RMSE) and correlation (R^2) are evaluated (Fig. 8). These metrics are determined for different timescales: 10-min, hourly, daily and monthly. All metrics are normalized with respect to the real mean wind speed. These analyses are complemented with the Weibull distribution and the windrose, based on 10-min values.

The same metrics are employed for wind standard deviation, but only presented for 10-min values. In the case of turbulence intensity the validation is centered on the relationship between wind speed and this variable. Turbulence and wind are first plotted in an XY scatterplot.

Due to the large number of results for each site, these must be summarized. Four summarizing metrics are defined: Mean Bias (MB), Mean Absolute Bias (MAB), Mean RMSE (MRMSE) and Mean R^2 (MR^2) as explained in Fig. 8. Validation is divided into a set of blocks. In the first block the performance of Vortex-LES for simulating wind speed is discussed. In the second part, the turbulence skills are evaluated by two variables: wind standard deviation and turbulence intensity.

Vortex-LES validation: Results

The discussion of the results involves three variables of interest for the wind energy industry: wind speed, wind standard deviation and turbulence intensity. Further results can be found in Doubrawa et al. (2017a).

The study discusses wind speed at length. First, the metrics for this variables are presented. This analysis includes different temporal frequencies: 10-min, hourly, daily and monthly averages.

Subsequently, the study discusses the daily cycle (i.e. stability regimes), latitudinal and seasonal behaviors.

Finally, a futher discussion is presented including the Weibull distribution, the energy spectrum and wind direction.

The discussion of standard deviation and turbulence intensity focuses on 10-min values. For wind standard deviation the discussion is centered on metrics, whilst the analysis of turbulence intensity is oriented towards characterisation of the site turbulence for wind turbine class selection (Fig. 8).

Wind speed: 10-min

The validation of wind speed time series shows a high dependence upon geographical features as well as on timescales (Tables 1, 2 and 3).

The analysis of 85 sites used for this validation reveals MAB of 5.1% ± 3.0% with respect to mean wind speed. The lowest value is found at the offshore sites with a 1.1% ± 0.5%, followed by the flat-terrain sites, with a MAB of 4.7% ± 2.7%. The forested sites show a similar MAB, with values of 4.7% ± 3.2%. Finally, complex-terrain locations experience the highest MAB, with 5.8% ± 2.8% (Table 1).

> *10-min time-series for 85 sites show a mean absolute bias of 5.1% and a mean R^2 of 0.683. The highest performance is produced at the offshore and the flat-terrain sites, while the complex-terrain sites experience a decrease in accuracy.*

The average MB for all sites is slightly positive: +1.3% ± 4.1%. This metric shows the lowest value at the offshore locations, with +0.8% ± 0.6% and the highest value at the complex-terrain and forested sites, with values ranging from +2.3% to +2.4%. The flat-terrain locations exhibit the reverse pattern. In general, these sites experience an underestimation of mean wind speed with values of -0.5% ± 3.9%.

The study of the MRMSE provides a result of 32.9% ± 5.1% with respect to mean wind speed. As with MAB, the offshore sites present the lowest MRMSE, with values of 17.6% ± 1.0%. The flat-terrain locations show a MRMSE of 31.4% ± 4.5%. Finally, the forested sites and complex-terrain sites reveal a similar MRMSE, with a mean value of 33.8% ± 5.3% and 34.7% ± 5.2%, respectively.

The results for MR^2 reveal a similar behavior to that described for the previous metrics. On average, Vortex-LES shows a 10-min MR^2 of 0.683 ± 0.052. The highest correlation is obtained at the offshore sites with 0.902 ± 0.026, while the lowest correlation is found at the complex-terrain locations, with 0.671 ± 0.059. The flat-terrain sites and forested sites exhibit intermediate results, with a correlation of 0.678 ± 0.039 and 0.690 ± 0.049, for each case.

> *The highest R^2 is obtained at the offshore sites, with 0.902, while the lowest one is provided by the flat-terrain sites, with 0.678.*

Wind speed: hourly, daily monthly averages

Analysis of the Vortex-LES time series at a lower frequency (hourly, daily and monthly scales) shows that MRMSE and MR^2 tend to improve (Table 1).

On average, Vortex-LES reveals a mean hourly MRMSE of 31.1% ± 5.1%, decreasing to 19.5% ± 4.4% and 11.1% ± 4.0% in daily and monthly averages, respectively. MR^2 increases from 0.684 ± 0.052 in hourly values to 0.881 ± 0.086 for monthly means.

MRMSE at the offshore sites decreases to 16.4% ±

Vortex-LES shows a mean hourly MRMSE of 31.1% ± 5.1% decreasing to 19.5% ± 4.4% and 11.1% ± 4.0% in daily and monthly averages, respectively. MR^2 increases from 0.684 ± 0.052 in hourly values to 0.881 ± 0.086 for monthly means.

Table 1: Summary of the wind-speed metrics

		MB (%)	MAB (%)	MRMSE (%)	R^2
All (100%)	10-min	+1.3 ± 4.1	5.1 ± 3.0	32.9 ± 5.1	0.683 ± 0.052
	Hourly			31.1 ± 5.1	0.684 ± 0.052
	Daily			19.5 ± 4.4	0.865 ± 0.047
	Monthly			11.1 ± 4.0	0.881 ± 0.086
Offshore (2%)	10-min	+0.8 ± 0.6	1.1 ± 0.5	17.6 ± 1.0	0.902 ± 0.026
	Hourly			16.4 ± 1.1	0.921 ± 0.025
	Daily			9.5 ± 0.6	0.949 ± 0.008
	Monthly			4.1 ± 0.3	0.965 ± 0.017
Flat (38%)	10-min	-0.5 ± 3.9	4.7 ± 2.7	31.4 ± 4.5	0.678 ± 0.039
	Hourly			29.9 ± 4.6	0.713 ± 0.040
	Daily			18.1 ± 4.1	0.868 ± 0.033
	Monthly			9.7 ± 3.1	0.863 ± 0.076
Complex (33%)	10-min	+2.3 ± 4.4	5.8 ± 2.8	34.7 ± 5.2	0.671 ± 0.059
	Hourly			33.0 ± 5.2	0.709 ± 0.060
	Daily			21.2 ± 4.5	0.854 ± 0.033
	Monthly			12.7 ± 4.7	0.858 ± 0.069
Forest (27%)	10-min	+2.4 ± 4.3	4.7 ± 3.2	33.8 ± 5.3	0.690 ± 0.049
	Hourly			32.0 ± 5.2	0.731 ± 0.047
	Daily			20.5 ± 4.6	0.869 ± 0.029
	Monthly			11.5 ± 4.2	0.930 ± 0.037

1.1% for hourly means, 9.5% ± 0.6% for daily averages and 4.1% ± 0.3% for monthly values. The correlation increases to 0.921 ± 0.025, 0.949 ± 0.008 and 0.965 ± 0.017 for each one of the temporal averages.

In the flat-terrain locations, MRMSE decreases to 29.9% ± 4.6% in hourly means, 18.1% ± 4.1% in daily means and 9.7% ± 3.1% in monthly results. The mean correlation improves from 0.713 ± 0.040, 0.868 ± 0.033 and 0.863 ± 0.076, respectively.

In the complex-terrain sites, MRMSE improves to 33.0% ± 5.2%, 21.2% ± 4.5% and 12.7% ± 4.7% in hourly, daily and monthly outcomes. The correlation increases from 0.709 ± 0.060 to 0.858 ± 0.069, with similar results in the daily and monthly means.

Finally, MRMSE in the forested locations decreases to 32.0% ± 5.2% in hourly means, 20.5% ± 4.6% in daily averages and 11.5% ± 4.2% in monthly ones. The average for all sites for MR^2 increases from 0.731 ± 0.047 in hourly means to 0.930 ± 0.037 in monthly means.

The correlation for 10-min time series is lower than for lower frequency datasets due to the high non-linear relationships in the atmosphere. Turbulent time series have a high degree of uncertainty because turbulence is not deterministic. Consequently, the temporal coherence is affected, although the results are good for the other metrics. Therefore, R^2 does not really constitute a good tool for evaluating the 10-min time series.

On the contrary, for lower-frequency outcomes, mesoscale and synoptic patterns driven by the reanalysis model arise, significantly increasing the correlation.

Wind speed: daily-cycle

Analysis of the day-night patterns shows that Vortex-LES provides better results during the daytime than at nighttime (Table 2, Fig. 9).

The average for all sites shows a mean daytime metric of +0.3 % ± 4.2% for MB, 5.4% ± 2.8% for MAB, 32.1% ± 4.7% for MRMSE and 0.699 ± 0.052 for MR^2. At night MB, MAB and MRMSE rise to +2.3% ± 4.5%, 5.5% ± 3.7% and 33.7% ± 5.6%, respectively. The correlation decreases to 0.667 ± 0.060.

The two offshore sites analyzed in the present paper reveal an inverse pattern. In general terms, MB, MAB and MR^2 perform better at night than in the daytime. MRMSE is an exception, providing similar results in

Table 2: Summary of the wind-speed day-night metrics

		MB (%)	MAB (%)	MRMSE (%)	R^2
All (100%)	Day	+0.3 ± 4.2	5.4 ± 2.8	32.1 ± 4.7	0.699 ± 0.052
	Night	+2.3 ± 4.5	5.5 ± 3.7	33.7 ± 5.6	0.667 ± 0.060
Offshore (2%)	Day	+0.9 ± 0.8	1.0 ± 0.8	17.6 ± 1.1	0.951 ± 0.027
	Night	+0.6 ± 0.3	0.9 ± 0.3	17.6 ± 0.9	0.968 ± 0.025
Flat (38%)	Day	-1.8 ± 3.5	5.4 ± 2.2	30.6 ± 4.1	0.687 ± 0.046
	Night	+1.0 ± 5.0	5.3 ± 4.1	32.4 ± 5.2	0.666 ± 0.042
Complex (33%)	Day	+1.2 ± 4.8	6.3 ± 3.2	33.8 ± 4.8	0.695 ± 0.053
	Night	+3.4 ± 4.4	6.4 ± 3.6	35.7 ± 5.9	0.644 ± 0.068
Forest (27%)	Day	+1.9 ± 3.8	4.7 ± 2.9	33.3 ± 5.1	0.695 ± 0.052
	Night	+2.9 ± 3.9	5.2 ± 3.5	34.5 ± 5.6	0.668 ± 0.063

Analysis of day-night patterns shows that Vortex-LES performs better in the daytime than at nighttime.

Average of 10-min series for all sites shows a R^2 of 0.699 ± 0.052 and 0.667 ± 0.060 for day and night, respectively.

the day and at night. Nevertheless, these results cannot be considered as statistically representative due to the low number of cases.

The flat-terrain sites exhibit two patterns that differ between day and night. During the daytime, Vortex-LES underestimates wind speed, with a MB of -1.8% ± 3.5%, whereas at night this metric drifts from negative to slightly positive values, with +1.0% ± 5.0%. MAB shows small variations from daytime to nighttime. MRMSE and MR^2 provide better results in the day with 30.6% ± 4.1% and 0.687 ± 0.046 than at night, with 32.4% ± 5.2% and 0.666 ± 0.042.

a) Offshore

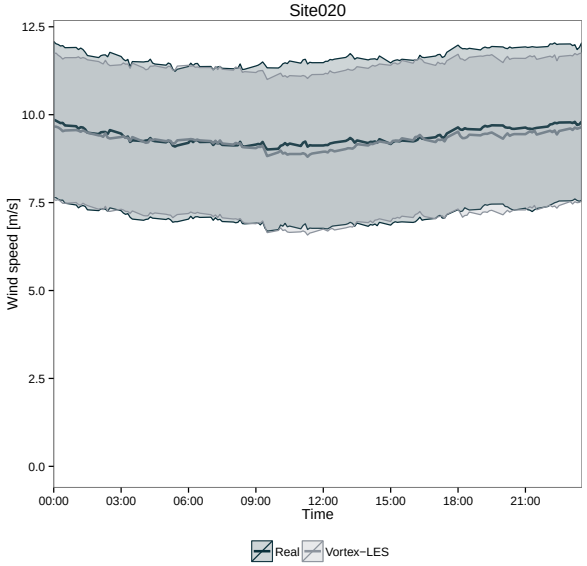

c) Complex-terrain

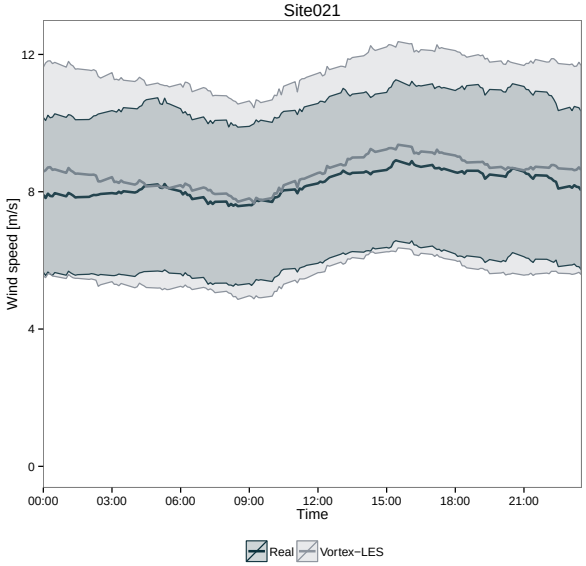

b) Flat-terrain

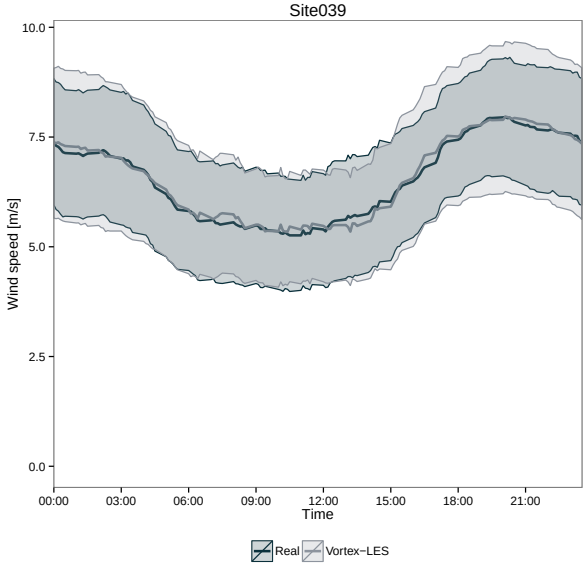

d) Forested

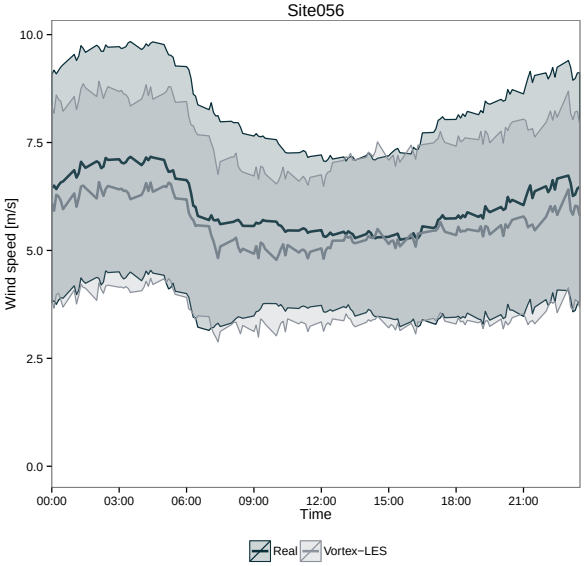

Fig. 9: Examples of the results of a typical day of wind speed for each of the proposed categories. The points indicate the 1-year averaged value for the 10-min interval and the bars show the standard deviation of the values.

The complex-terrain and forested sites show the same behavior that flat-terrain locations but they present a positive MB during the daytime period.

Fig. 9 illustrates these results in four examples, each one for a different type of site.

Wind speed: spatial classification

In this section, sites have been clustered in three regions defined in terms of latitude. In the Northern Hemisphere, tropical zones are defined from 0° to 30°, mid-latitude areas from 30° to 60° and polar regions from 60° to 90°. The same thresholds are used in the Southern Hemisphere but in negative values. Separation of the Northern and Southern Hemispheres is not considered due to the lack of sites in the Southern one. This kind of discussion merits further study. As it was previously introduced, this analysis is performed with 16 tropical sites (i.e. 19%), 65 mid-latitude sites (76%) and 4 polar sites (5%).

Analysis by groups (Table 3) reveals that the polar sites exhibit the lowest MRMSE and the highest MR^2. In these sites, MR^2 is 0.783 ± 0.017 for 10-min time series, 0.836 ± 0.013 for hourly outcomes, 0.895 ± 0.008 for daily values and 0.895 ± 0.069 for monthly ones. As expected from the previous sections, the MRMSE is maximum for 10-min time series with 25.3% ± 1.7% and decreases to 7.4% ± 2.3% in monthly averages. These sites experience the most negative MB with -2.4% ± 3.7% and a MAB of 5.3% ± 2.3%.

The mid-latitude sites present an intermediate MR^2 and MAB. In the case of MR^2, with 0.708 ± 0.047 for 10-min time series, increasing to 0.874 ± 0.062 for monthly averages. All these sites show a MAB of 5.0% ± 3.2 %. In contrast to polar sites, these sites show an overestimation of mean wind speed with a MB of +1.8% ± 4.1%.

> *The mid-latitude sites provide an intermediate results for MR^2 and MAB with 0.708 and 5.0%, respectively.*

Table 3: Summary of the wind-speed metrics by region

		MB (%)	MAB (%)	MRMSE (%)	R^2
Tropical (19%)	10-min	-0.1 ± 4.1	4.9 ± 2.8	32.3 ± 4.9	0.571 ± 0.046
	Hourly			30.9 ± 5.2	0.608 ± 0.046
	Daily			18.7 ± 4.9	0.802 ± 0.045
	Monthly			10.5 ± 3.3	0.861 ± 0.041
Mid-latitude (76%)	10-min	+1.8 ± 4.1	5.0 ± 3.2	33.5 ± 5.2	0.708 ± 0.047
	Hourly			31.7 ± 5.1	0.744 ± 0.046
	Daily			20.0 ± 4.4	0.878 ± 0.027
	Monthly			11.3 ± 4.3	0.874 ± 0.062
Polar (5%)	10-min	-2.4 ± 3.7	5.3 ± 2.3	25.3 ± 1.7	0.783± 0.017
	Hourly			23.4 ± 1.9	0.836 ± 0.013
	Daily			15.8 ± 2.3	0.895 ± 0.008
	Monthly			7.4 ± 2.3	0.895 ± 0.069

Table 4: Summary of the wind-speed metrics by season

		MB (%)	MAB (%)	MRMSE (%)	R^2
All (100%)	Winter	+3.4 ± 5.0	6.9 ± 3.9	35.8 ± 5.1	0.663 ± 0.079
	Spring	+0.9 ± 4.4	5.4 ± 3.0	32.8 ± 5.1	0.653 ± 0.073
	Summer	-0.9 ± 4.3	5.1 ± 3.0	29.4 ± 4.5	0.637 ± 0.061
	Fall	+1.3 ± 4.6	6.3 ± 3.5	31.6 ± 5.2	0.670 ± 0.068
Tropical (19%)	Winter	-0.9 ± 5.3	6.6 ± 3.5	34.4 ± 5.1	0.518 ± 0.079
	Spring	-0.9 ± 3.3	5.0 ± 1.4	30.1 ± 3.6	0.514 ± 0.089
	Summer	-1.4 ± 4.3	5.3 ± 3.0	28.4 ± 3.8	0.541 ± 0.059
	Fall	-1.4 ± 2.8	3.5 ± 2.1	29.3 ± 3.4	0.528 ± 0.068
Mid-latitude (76%)	Winter	+4.6 ± 4.5	7.1 ± 4.1	36.7 ± 6.5	0.694 ± 0.074
	Spring	+1.6 ± 4.5	5.4 ± 3.3	33.8 ± 5.9	0.675 ± 0.065
	Summer	-0.7 ± 4.4	5.1 ± 3.2	30.1 ± 4.6	0.654 ± 0.059
	Fall	+2.0 ± 4.8	5.6 ± 3.8	32.6 ± 5.6	0.694 ± 0.062
Polar (5%)	Winter	-0.7 ± 3.6	4.2 ± 2.0	25.3 ± 0.9	0.760 ± 0.021
	Spring	-3.0 ± 4.0	6.4 ± 2.2	27.1 ± 2.0	0.794 ± 0.019
	Summer	-2.7 ± 2.6	4.4 ± 2.1	22.9 ± 1.4	0.677 ± 0.044
	Fall	-1.1 ± 4.0	5.2 ± 2.0	23.9 ± 1.2	0.785 ± 0.037

Finally, tropical sites show the lowest MR^2 values, ranging from 0.571 ± 0.046 for 10-min series to 0.861 ± 0.040 in monthly means. MRMSE produces an intermediate performance ranging from 32.3% ± 4.9% to 10.5% ± 3.3%. MAB is similar to the mid-latitude sites with 4.9% ± 2.8%. In terms of bias, they reveal a near-zero MB of -0.1% ± 4.1%.

This variation of the results is driven by the reanalysis dataset. In the tropical sites, the main variations in wind speed are produced by local effects and seasonal patterns (e.g. Monsoon). This produces the significant increment of MR^2 detected from hourly to daily time series and from hourly to monthly ones. Furthermore, wind speed during the day is driven by high convection proccesses breaking down the main signal and reducing the correlation in 10-min and hourly values.

The mid-latitude sites are driven by synoptic regimes, leading to higher correlation in all scales. The overestimation of wind speed is a consequence of the reanalysis dataset, promoted by the increment in resolution.

Finally, polar sites exhibit behavior similar to the mid-latitude locations but they are affected by stability. Stable regimes lead to strong wind profiles. However, these regimes are not well resolved in atmospheric models, thus giving rise to the observed underestimation of wind speed.

Wind speed: seasonal results

The seasonal discussion of Vortex-LES is performed by dividing the 10-min time series in four blocks: winter, spring, summer and fall. In the Northern Hemisphere winter is the result of grouping into

Winter and fall achieve the highest correlation, with an average of 0.663 and 0.670.

December - January - February (DJF), spring is March - April - May (MAM), summer is June - July - August (JJA) and fall is September - October - November (SON). The pattern is reversed in the Southern Hemisphere, with winter as (JJA), spring as (SON), summer as (DJF) and fall as (MAM).

The average for all sites shows that winter and fall achieve the highest correlation with 0.663 ± 0.079 and 0.670 ± 0.068, respectively, while summer reaches the lowest value with 0.637 ± 0.061 (Table 4). MAB and MRMSE are minimum in summer, with 5.1% ± 3.0% and 29.4% ± 4.5%, increasing in fall and spring and reaching the highest value in winter, with 6.9% ± 3.9% and 35.8% ± 5.1%. Vortex-LES 10-min outcomes tend to overestimate wind speed in winter, with an MB of 3.4% ± 5.0%, decreasing in fall and spring and drifting from positive to slightly negative values in summer, with -0.9% ± 4.3%.

From the discussion presented in the previous section one may conclude that merging all sites in the seasonal analysis is not a good option for an in-depth discussion and hence, the same analysis by latitudes has been introduced herein.

The metrics for the tropical sites respond to two well-defined seasonal patterns: winter-spring and summer-fall. In the former the correlation is minimum and MAB is maximum, with values ranging from 0.514 ± 0.089 to 0.518 ± 0.079 and from 5.0% ± 1.4% to 6.6% ± 3.5%, respectively. In the latter the correlation increases to values between 0.528 ± 0.068 and 0.541 ± 0.059. The MAB in summer shows similar values to those of the above mentioned seasons, while in fall it decreases to 3.5% ± 2.1%.

The mid-latitude sites show the highest correlation in winter and fall, with values around 0.694 due to the storm-track activity clearly defined by the reanalysis. On the contrary, spring and summer exhibit a decrease of the MR^2 due to decreased activity in the synoptic patterns and the appearance of local effects (e.g. sea breezes). The highest MAB is experienced in winter, with 7.1% ± 4.1%, spring and fall show similar outcomes, with 5.4% ± 3.3% and 5.6 ± 3.2%. Finally, the highest performance is observed in summer with 5.1% ± 3.2%. Wind speed is overestimated in all seasons with the exception of summer.

In the polar sites, the highest correlation is produced in spring and fall, with values around 0.790. The lowest values are obtained in summer, with 0.677 ± 0.044. Winter is an intermediate case. The highest MAB is observed in spring, with 6.4% ± 2.2% while the lowest one is observed in winter and summer, with 4.2% ± 2.0% and 4.4% ± 2.1%, respectively. Wind speed is overestimated in all seasons.

Wind speed: Weibull distribution

The Weibull parameters show a good agreement between observed and modeled wind distributions. Generally, Vortex-LES simulations reproduce all wind regimes, being calms and extreme events, thus constituting big improvements with respect to mesoscale simulations.

The validation focuses on two parameters: relative error in the scale parameter A and relative error in the shape parameter k. Table 5 shows a summary of the metrics for all sites and by the different categories aforementioned. Fig. 10 shows four

Table 5: Summary of Weibull parameters

		A (%)	k (%)
All (100%)	10-min	1.1 ± 5.1	3.2 ± 5.5
Offshore (2%)	10-min	4.7 ± 0.1	1.5 ± 0.7
Flat (38%)	10-min	0.7 ± 5.1	-0.8 ± 5.0
Complex (33%)	10-min	3.2 ± 5.9	6.0 ± 6.3
Forest (27%)	10-min	-1.3 ± 3.3	-5.6 ± 4.9

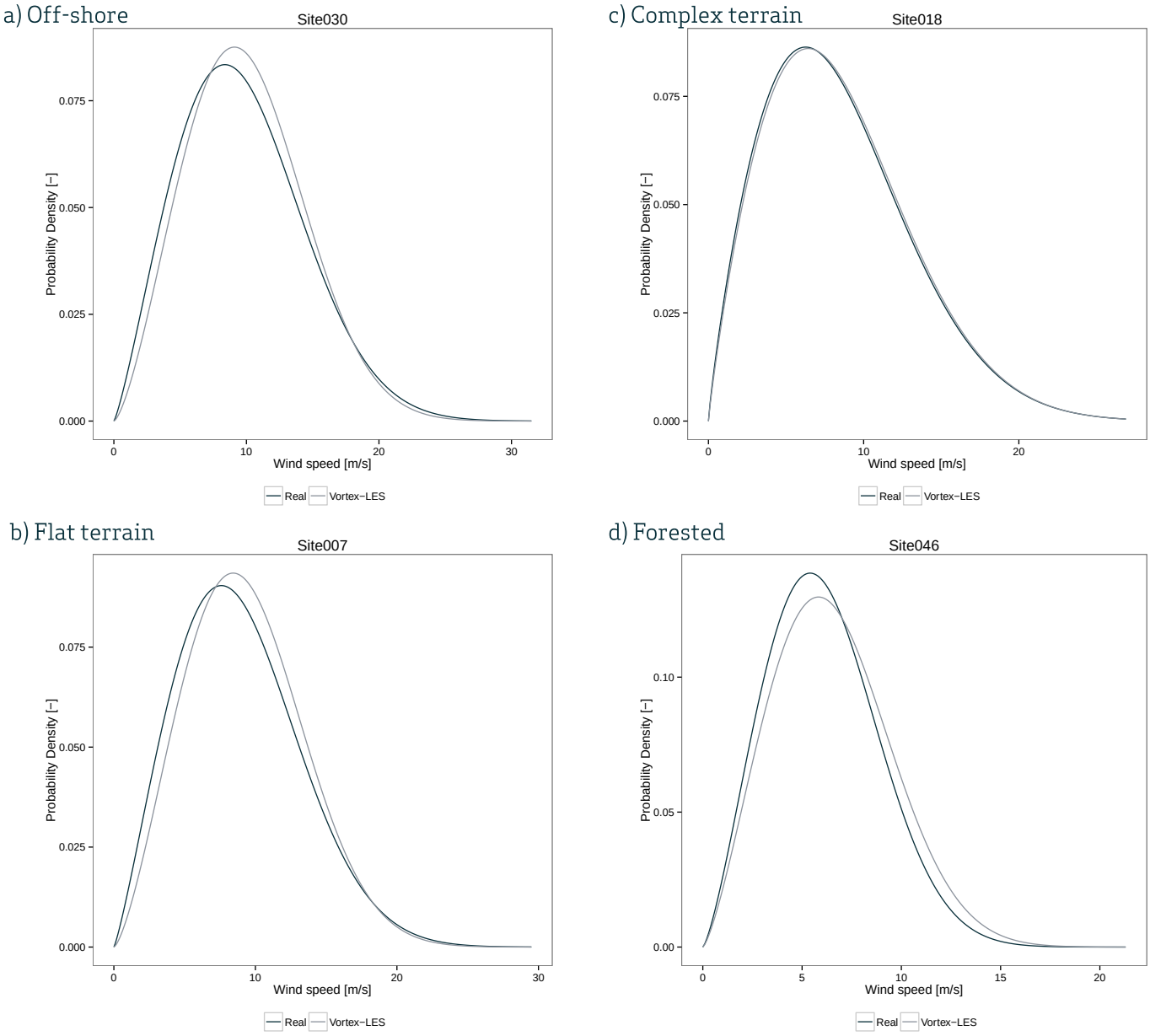

Fig 10: Example of a comparison between the Weibull distribution for the measurements and Vortex-LES for different cases.

The Weibull parameters A and k are estimated with a mean relative error of 1.1% and 3.2%, respectively.

Vortex-LES reproduces all the wind regimes with high accuracy, particularly extreme events.

samples of the results for four sites.

The averaged error for all sites is +1.1% ± 5.1% and +3.2% ± 5.5% for A and k, respectively.

The offshore sites present a high error in A with +4.7% ± 0.1% and a small deviation in k +1.5% ± 0.7.

The flat-terrain sites show the lowest error, with +0.7% ± 5.1% -0.8 ± 5.0 for A and k. The complex-terrain sites increase errors in both A and k, with a clear overestimation of 3.2% ± 5.9% and 6.0% ± 6.3%.

Finally, the forested sites show an underestimation of these parameters with errors of -1.3% ± 3.3% and -5.6% ± 4.9%.

Wind speed: vertical profiles

In general terms, there is either a limited number of sites with measurements at more than one height or the clients do not share the datasets with us. Consequently, the analysis of the vertical profiles is reduced to 7 of the 85 sites used in this validation. Specifically, these localities are Site 2, Site 7, Site028, Site 30, Site 38, Site 45 and Site 50 (Table 6).

Table 6: Summary of the vertical levels used for the validation of the vertical profiles

Site	Heights with available real measurements
Site002	10, 20, 40, 80 m
Site007	20, 30, 40, 50, 60 m
Site028	60, 80, 100 m
Site030	33, 40, 50, 60, 70, 80, 90, 100 m
Site038	20, 30, 50, 70 m
Site045	40, 50, 60 m
Site050	30, 35, 50, 100 m

Analysis of the vertical profiles is performed by comparing the real and modeled wind shears based on a log fit, as

$$\log(V_1/V_2) = \alpha \log(z_1/z_2) \qquad (1)$$

V_1 and V_2 being the annual mean wind speed at two different heights, z_1 and z_2, and the shear coefficient, α, respectively.

An example of this fit is illustrated with two examples in the complex-terrain and in the offshore sites in Fig. 11.

All sites show a similar behavior, the bias tends to be positive close to the surface, drifting to near-zero or slightly negative values at the upper levels.

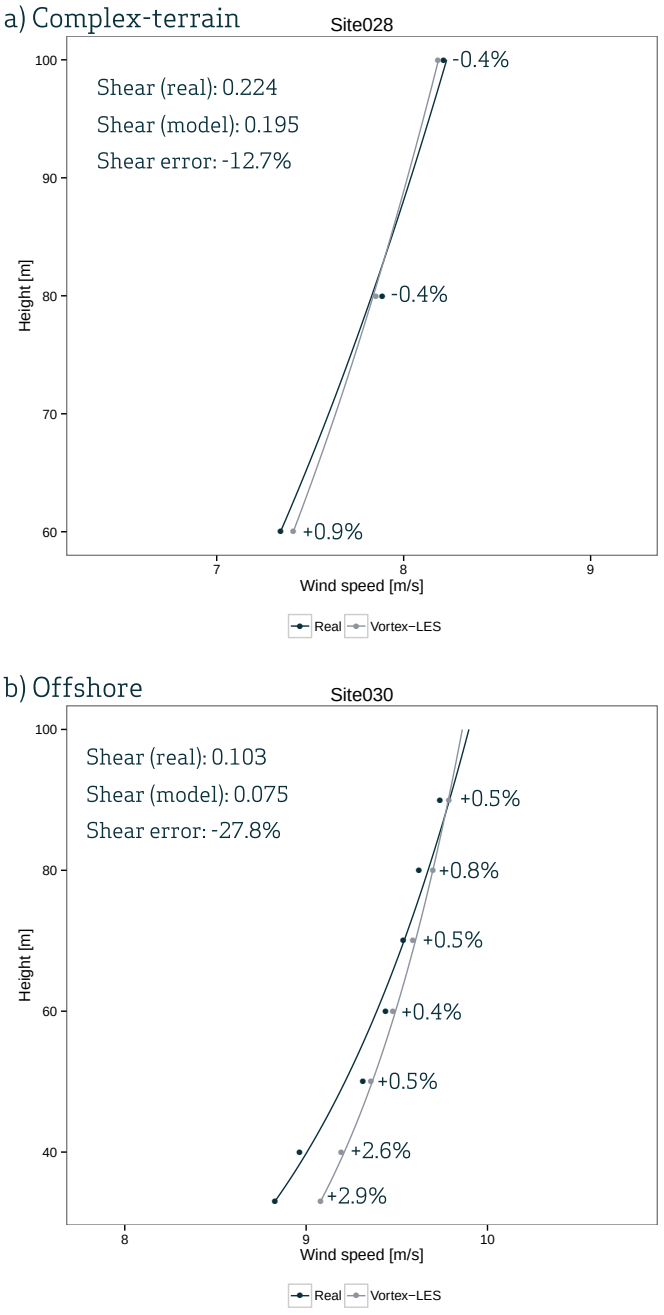

Fig. 11: Analysis of the wind profile for a site in a complex-terrain site (left-hand plot) and an offshore site (right-hand plot). The numbers indicate the anual bias at each height normalized with respect to the real mean wind speed.

The physical reason for these patterns can be found in the surface features. The first levels of the real atmosphere are highly perturbed by the local features (trees, buildings or waves, among others), that cannot be resolved by the Vortex-LES at 100 m. The model parameterizes these effects by assuming some precomputed roughnesses, sufficient for mesoscale applications, but more important in the

case of microscale simulations. Consequently, the model shows a tendency to overestimate the lower levels. Nonetheless, these levels have a minor impact in the wind industry and it is an issue that will be resolved during the coming years, as this new approach penetrates into the market.

The higher levels (i.e. between 50 and 100 m above the ground) are less affected by the surface characteristics, and thus, the bias decreases significantly.

Below 50 m, the bias fluctuates between +5 and +20% with respect to the mean wind speed, while between 50 and 100 m the bias ranges between -5% and +5%, although in some cases it reaches values of approximately 10%.

This bias in wind speed is propagated to the wind shear, leading to an averaged relative error ranging from -20% to +20%.

Energy spectrum

Spectral analysis of the Vortex-LES time series shows a similar behavior in all sites, thus solving the problem of the mesoscale simulations for motions with a characteristic time scale lower than 1 h.

Large scales are provided by the global reanalysis used for the simulation initialization. These scales are generally well reproduced by the resolution of these models.

Eddies with a lifetime between one hour and one day are introduced by the mesoscale model as shown in Fig 12. However, as discussed in Why Vortex-LES?, the grid resolution used in these simulations is not valid with regard to resolving the whole spectrum at frequencies higher than 10^{-3} Hz (i.e. lower than 1 h), producing a strong decay of the energy .

Coupling a LES algorithm in a mesoscale model to solve the microscale makes a great improvement in the energy cascade.

Generally, a similar behavior is observerd in all sites.

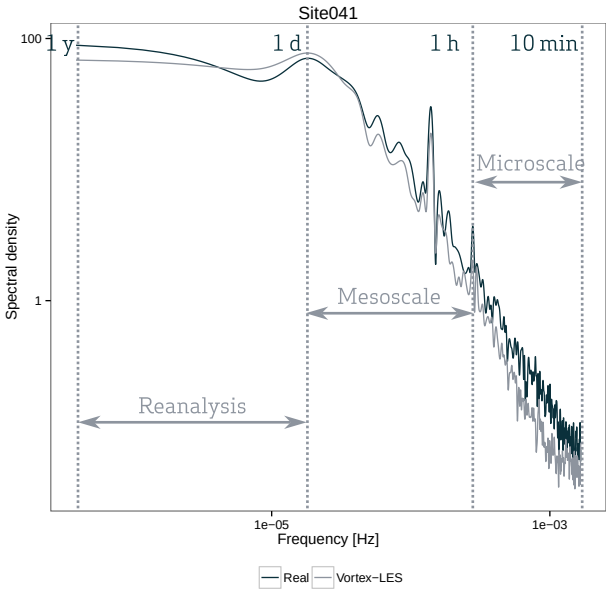

Fig 12: Example of the energy spectrum for the Site041. The dashed lines indicates the time scale associated to the motions.

For frequencies with an order of magnitude of 10^{-3} Hz, the Vortex-LES time series reproduces a slope similar to that of the real measurements but with a significant underestimation of the energy.

This issue is a consequence of the Terra Incognita issue, which requires further research in order to be solved.

On the contrary, the energy associated with the highest-frequency events (i.e. 10^{-2} Hz) is well simulated and in some cases, slightly overestimated.

Wind direction

Validation of the wind direction shows an averaged bias of 3º and a mean MAE of 18º, less than one wind rose sector (Table 7). The preformance is similar for the offshore, flat-terrain and complex-terrain sites, with a mean MAE of around 34º. In the offshore sites, the wind direction is slightly underestimated, with -2º, while the complex-terrain sites show a slightly positive bias of +2º. Finally, the flat-terrain sites produce a near-zero bias.

The larger mean bias is observed in the complex-terrain sites, forest sites and complex-terrain and

Table 7: Summary of the wind-direction metrics

		Bias (deg)	MAE (deg)
All (100%)	10-min	3	35
Offshore (2%)	10-min	-2	18
Flat (38%)	10-min	0	34
Complex (33%)	10-min	2	34
Forest (27%)	10-min	10	31

forest sites with +10°. However, the mean MAE is significantly lower, with 31°.

Fig. 13 shows an example of two wind roses, one for site 16 and the other one for site 78.

The mean bias and MAE for the 85 sites in the wind direction are +3° and 18°, respectively.

Fig 13: Example of the wind roses for two sites.

Wind standard deviation

High frequency wind-speed variations (i.e. higher than 10-min) represented by wind standard deviation, correspond to the Fluid Dynamics field and hence, they are intrinsically related with wind speed. For this reason, the validation in this section focuses upon 10-min time series, and other spatial and temporal analysis are therefore not provided.

Wind standard deviation is slightly overestimated, with a MB of +0.6% ± 0.8%, increasing to 1.3% ± +0.6% and 6.6% ± 0.9% for MAB and MRMSE, respectively.

On average (Table 8), wind standard deviation is slightly overestimated, with a MB of +0.6% ± 0.8%, increasing to 1.3% ± 0.6% and 6.6% ± 0.9% for MAB and MRMSE, respectively. All sites show similar errors. The lowest MAB and MRMSE are achieved at offshore locations with 0.3% ± 0.0% and 4.3% ± 0.2%, increasing to 1.1% ± 0.3% and 5.8% ± 0.5% in flat-terrain, 1.3% ± 0.6% and 7.0% ± 0.8% in complex-terrain and 1.6% ± 1.1% and 7.4% ± 1.2% in forested zones.

The temporal coherence of the modeled outcomes is more difficult to achieve because standard deviation is a second order variable and turbulence can be considered as a stochastic phenomenon. On average, MR^2 for all sites is 0.288 ± 0.055. This magnitude is maximum at the forested sites with 0.307 ± 0.069 and it shows similar results for the other kind of sites, with values of around 0.285.

Vortex-LES is able to capture the diurnal cycle of the PBL structure with stable layers at night and convection during the day.

Analysis of the day-night patterns (Fig. 14) shows that Vortex-LES is capable of capturing the diurnal cycle of the PBL structure with stable layers at night

Table 8: Summary of the standard-deviation metrics

		MB (%)	MAB (%)	MRMSE (%)	R^2
All (100%)	10-min	+0.6 ± 0.8	1.3 ± 0.6	6.6 ± 0.9	0.288 ± 0.055
Offshore (2%)	10-min	+0.3 ± 0.0	0.3 ± 0.0	4.3 ± 0.2	0.291 ± 0.066
Flat (38%)	10-min	+0.8 ± 05	1.1 ± 0.3	5.8 ± 0.5	0.284 ± 0.029
Complex (33%)	10-min	+0.4 ± 0.9	1.3 ± 0.6	7.0 ± 0.8	0.281 ± 0.068
Forest (27%)	10-min	+0.6 ± 1.3	1.6 ± 1.1	7.4 ± 1.2	0.307 ± 0.069

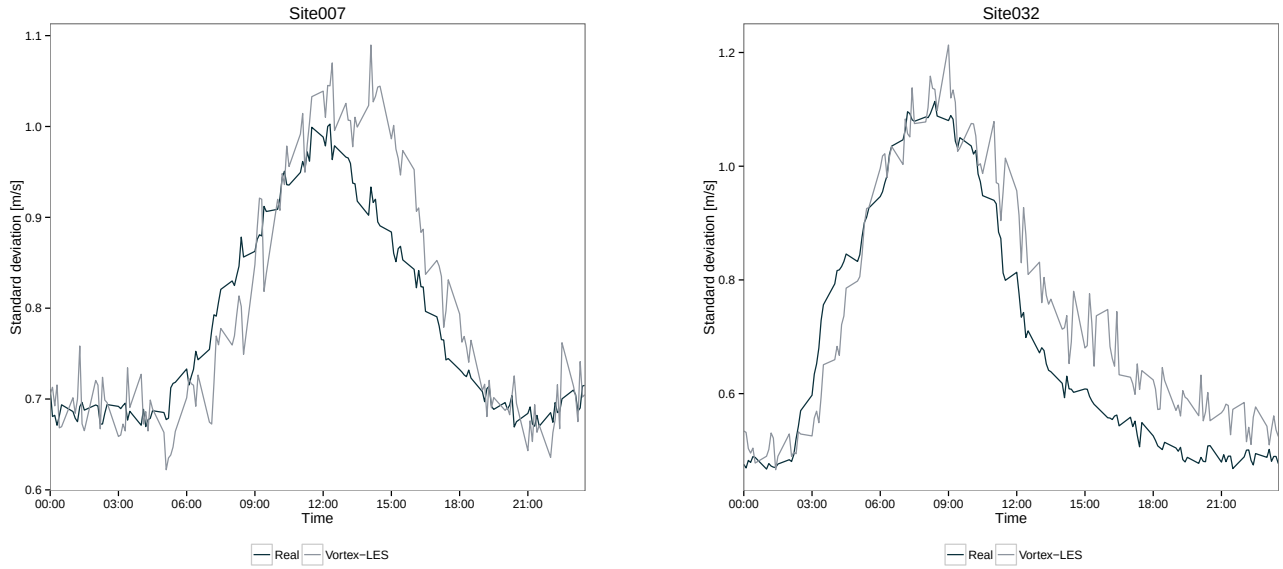

Fig 14: Example of the standard-deviation output for a typical day.

and convection during the day. Nevertheless, a shift is observed a shift both in warming and cooling. Vortex-LES generally experiences a delay in the increment in turbulence during the first part of the day and a delay in the decrease in turbulence after noontime.

This issue is related with the surface layer scheme and constitutes a common problem in all NWP models. In this sense, the surface layer parameterization needs to be revised in the future, as previously indicated.

Turbulence Intensity

The error in the turbulence intensity is made up of the errors both in mean and standard deviation. Consequently, the correlation driven by the temporal coherence of the time series is apparently low. However, unlike wind speed or other meteorological fields, the interest of this magnitude does not involve the temporal description of the site. The main interest of the turbulence intensity is seen in the turbulent characterization of the site in terms of the curves defined by the International Electrotechnical Commission (IEC). For this reason the validation of

the turbulence intensity focuses upon the relationship between this variable and wind speed, as shown in Fig. 15.

The $MMAE_w$ for all sites is 1.8% ± 0.5%, while the mean error in $MMAE_{15}$ is 1.9% ± 0.6%, both defined in units of TI (Table 9).

Fig 15 shows three examples of the results in TI-wind speed.

Table 9: Summary of the TI metrics

	$MMAE_w$ (%)	$MMAE_{15}$ (%)
TI	1.8 ± 0.5	1.9 ± 0.6

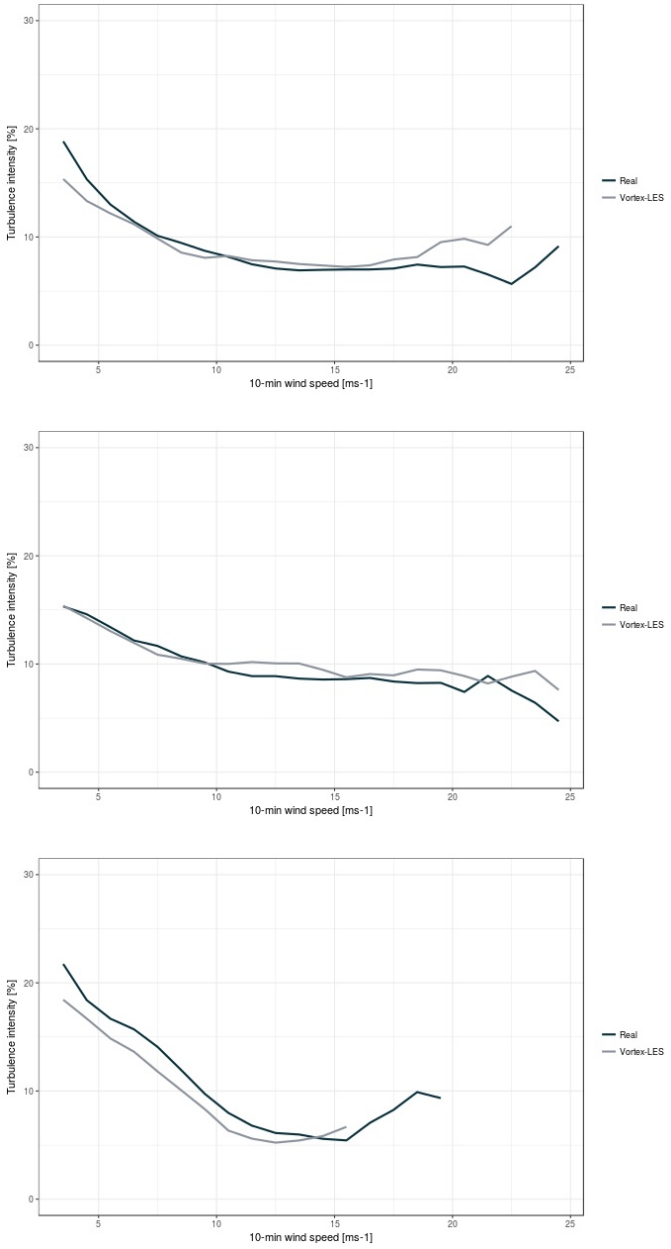

Fig 15: Example of IEC curves from measurements and Vortex-LES outcomes.

Conclusions

The present document describes the implementation and performance of the Vortex-LES product (Fig. 3). The approach presented employs the WRF-LES model adapted for real simulations.

The new version of the model includes two main improvements: one in the treatment of the LBC (Fig. 4) and the other one in the computation resources.

Vortex-LES achieves a resolution of 100 m and it produces one year of 10-min time series at any location (Fig. 5). This resolution will be increased in the coming years.

The output of the model is saved every 0.25 s and then post-processed to 10-mean averages, fluxes and standard deviations (Fig. 6). This process is performed for all fields in a region between the surface and 200 m covering an area of 2 km x 2 km. Indeed, Vortex-LES functions as a "poor" sonic anemometer which allows new variables, such as wind gust, to be saved without additional parameterizations.

Vortex-LES has been validated in 85 sites for wind speed and 50 sites for wind standard deviation and turbulence intensity (Figs. 7 and 8).

For wind speed, the validation (Table 1) shows a mean absolute error of 5.1% ± 3.0% with respect to mean wind speed. The correlation is minimum for 10-min time series with 0.683 ± 0.052 and increases as the time frequency decreases, reaching 0.881 ± 0.086 in terms of monthly means. This behavior is associated

with two features: i) for 10-min values, stochastic patterns linked to turbulence are dominant, thus reducing the signal of the dataset and ii) as time frequency decreases, large scale patterns driven by the reanalysis appear, increasing the signal of the time series.

Furthermore, the information provided by the reanalysis dataset defines the performance of the Vortex-LES outcomes for different regions around the world (Table 3).

The main variations in tropics are produced by local effects and seasonal patterns. In terms of metrics, the correlation for 10-min and hourly values is significantly affected, with values lower than 0.608, whereas for daily and monthly averages it increases rapidly.

Mid-latitude and polar sites are driven by synoptic and mesoscale regimes leading to a significant increment in the correlation. 10-min time series show a correlation ranging from 0.650 to 0.750, increasing to 0.825 and 0.950 for monthly means. Polar sites generally tend to underestimate wind speed, as stability is dominant in these regions and constitutes a common issue in meteorological models as well as in LES algorithms.

Performance of the Vortex-LES results is also affected by the complexity of the site. In the present research, the complexity has been grouped into four categories: offshore, flat-terrain, complex-terrain and forested regions (Table 1). The most significant outcomes are provided by the offshore sites, as these are the simplest ones. Results decrease progressively in the flat-terrain, complex-terrain and forested sites. The forested sites show the highest overestimation of wind speed, with values of around +2.4% ± 4.3%, as in the current versions of NWP models, forests are not resolved and are simplified with a roughness value.

Study of the Weibull distribution shows good agreement with measurements. An important difference of Vortex-LES datasets with respect to the standard mesoscale outcomes refers to their capacity to distinguish and resolve calms and extreme events (Table 5, Fig 10).

Validation of wind standard deviation reveals a good degree of agreement with measurements (Table 8).

Values averaged for all sites show a mean absolute bias of 1.3% ± 0.6% with respect to mean wind standard deviation. This error is minimum in offshore sites, with 0.3% ± 0.0%, and maximum in forested sites, with 1.6% ± 1.1%.

The discussion of turbulence intensity focuses upon the turbulent characterization of the site (Figs. 8 and 15). The validation of the IEC curves shows a mean absolute error (Table 9) of around 1.8% ± 0.5% in units of turbulence intensity.

This is the first step towards achieving a seamless modeling chain across the scales, from large motions in the atmosphere to small eddies at the microscale. In the coming years, new improvements are to be expected, such as an increase in grid resolution to tens of meters, and Terra Incognita and surface layer parameterizations, among others.

References

Doubrawa, P., Montornès, A., Barthelmie, R. and Casso, P.: Effect of Wind Turbine Wakes on the Performance of a Real Case WRF-LES Simulation. Journal of Physics Conference Series 854(1):012010. 2017a.

Doubrawa, P. Montornès, A., Barthelmie, R.., Pryor, S. C. and Casso, P.: Analysis of different gray zone treatments in WRF-LES real case simulations (2017b, under revison)

Haupt, S. E., Shaw, W. J. and Kosovic, B.: The DOE A2e Mesoscale to Microscale Coupling Project. 22nd Symposium on Boundary Layers and Turbulence. 2016

Kosovic, B., Jiménez, P, Haupt, S. E., Olson, J. B., Bao, J. W., Grell, E. D. and Kenyon, J.: A Three-dimensional PBL Parameterization for High-resolution Mesoscale Simulation over Heterogeneous and Complex Terrain. AGU Fall Meeting Abstracts. 2016.

Mirocha, J., Branko K. and Gokhan K: Resolved

turbulence characteristics in large-eddy simulations nested within mesoscale simulations using the weather research and forecasting model. Monthly Weather Review 142.2, 806-831, 2014.

Montornès, A., Casso, P., Kosovic, B. and Lizcano, G.: Is WRF-LES a suitable tool for realistic turbulence analyses in wind resource assessment applications? 22nd Symposium on Boundary Layers and Turbulence. 2016.

Montornès, A., Casso, P., Kosovic, B. and Lizcano, G.: WRF-LES in 250+ real sites: Learnings and Challenges. 18th Annual WRF User's Workshop. 2017.

Muñoz-Esparza, D., Kosovic, B., Mirocha, J. and van Beeck, J.: Bridging the transition from mesoscale to microscale turbulence in numerical weather prediction models. Boundary-layer meteorology 153.3, 409-440. 2014.

Muñoz-Esparza, D., Kosovic, B., van Beeck, J. and Mirocha, J.: A stochastic perturbation method to generate inflow turbulence in large-eddy simulation models: Application to neutrally stratified atmospheric boundary layers. Physics of Fluids 27.3, 035102. 2015.

Shin, H. H. and Hong, S. Y.: Representation of the subgrid-scale turbulent transport in convective boundary layers at gray-zone resolutions. Monthly Weather Revision, 143, 250-271. 2015.

Skamarock, W. C., Klemp, J. B., Dudhia, J., Gill, D. O., Barker, D. M., Wang, W. and Powers, J. G.: A description of the Advanced Research WRF Version 3. NCAR Tech Notes-475+STR. 2008.

Udina Sistach, Mireia.: Modeling the atmospheric boundary layer in stably stratified conditions and over complex terrain areas: from mesoscale to LES. University of Barcelona. 2015.

Udina, M., Sun, J., Kosovic, B. and Soler, M. R.: Exploring Vertical Turbulence Structure in Neutrally and Stably Stratified Flows Using the Weather Research and Forecasting Large-Eddy Simulation (WRF-LES) Model. Boundary-Layer Meteorology 161.2, 355-374. 2016.

Talbot, C., Bou-Zeid, E. and Smith, J.: Nested mesoscale large-eddy simulations with WRF: performance in real test cases. Journal of Hydrometeorology 13.5, 1421-1441. 2012.

Warner, T. T.: Numerical weather and climate prediction. Cambridge University Press, 2010.

Wyngaard, J. C.: Toward numerical modeling in the Terra Incognita. Journal of the atmospheric sciences 61.14, 1816-1826. 2004.

Vortex's contributions

Montornès, A., Casso, P., Kosovic, B. and Lizcano, G.: Mesoscale-microscale coupling in real world: a new milestone in the wind energy industry. 4th International Conference of Energy. 2017.

Montornès, A., Casso, P., Kosovic, B. and Lizcano, G.: WRF-LES in 250+ real sites: Learnings and Challenges. 18th Annual WRF User's Workshop. 2017.

Montornès, A., Casso, P., Kosovic, B. and Lizcano, G.: Mesoscale-Microscale coupling: a new time for the atmospheric modeling. 6th Meteorology and Climatology of the Mediterranean. 2017.

Montornès, A., Casso, P., Kosovic, B. and Lizcano, G.: WRF-LES in the real world: Towards a seamless modeling chain for wind industry applications. 17th Annual WRF Users' Workshop. 2016.

Montornès, A., Casso, P., Kosovic, B. and Lizcano, G.: Is WRF-LES a Suitable Tool for Realistic Turbulence Analyses in Wind Resource Assessment Applications? 22nd Symposium on Boundary Layers and Turbulence (AMS). 2016.

Montornès, A., Casso, P. and Lizcano, G.: Towards a seamless modeling chain. publication description The European Wind Energy Association. 2015.

Montornès, A., Casso, P., Lizcano, G. and Moreno, P.: Towards next generation of wind resource modeled time-series. 3rd International Conference of Energy

and Meteorology. 2015.

Montornès, A., Casso, P. and Lizcano, G.: Can mesoscale models reach the microscale? EWEA Resource Assessment Workshop. 2015.